Glutamate Carboxypeptidase II: An Overview of Structural Studies and Their Importance for Structure-Based Drug Design and Deciphering the Reaction Mechanism of the Enzyme

J. Pavlíček, J. Ptáček and C. Bařinka*

Institute of Biotechnology, Academy of Sciences of the Czech Republic, Videnska 1083, 14200 Praha 4, Czech Republic

Abstract: Recent years witnessed rapid expansion of our knowledge about structural features of human glutamate carboxypeptidase II (GCPII). There are over thirty X-ray structures of human GCPII (and of its close ortholog GCPIII) publicly available at present. They include structures of ligand-free wild-type enzymes, complexes of wild-type GCPII/GCPIII with structurally diversified inhibitors as well as complexes of the GCPII(E424A) inactive mutant with several substrates. Combined structural data were instrumental for elucidating the catalytic mechanism of the enzyme. Furthermore the detailed knowledge of the GCPII architecture and protein-inhibitor interactions offers mechanistic insight into structure-activity relationship studies and can be exploited for the rational design of novel GCPII-specific compounds. This review presents a summary of structural information that has been gleaned since 2005, when the first GCPII structures were solved.

Keywords: Glutamate carboxypeptidase II, metallopeptidase, X-ray crystallography, prostate-specific membrane antigen, folate hydrolase.

1. INTRODUCTION

Human glutamate carboxypeptidase II (GCPII; E.C. 3.4.17.21) is a zinc-dependent exopeptidase with a broad pharmacological potential [1]. Two major areas of pharmacologic interventions are closely linked to two prominent sites of GCPII expression [2-5]. The CNS/PNS form of the enzyme, formerly termed N-acetylated-α-linked acidic dipeptidase (NAALADase), is a therapeutic target linked to neurologic disorders associated with acute or chronic glutamate excitotoxicity [6;7]. On the other hand, GCPII overexpressed in malignant prostatic human tissue, also known as prostate-specific membrane antigen (PSMA), is used as a marker for the imaging/therapy of prostate cancer, especially in case of advanced and metastatic disease [8,9]. In addition to prostate cancer, GCPII overexpression on the neovasculature of a variety of solid tumors expands therapeutic/diagnostic utility of the enzyme to a majority of solid cancers [10-12].

This review summarizes the literature body pertinent to the elucidation of the 3-dimensional structure of human GCPII (and its close homolog GCPIII) that has become available within the last 7 years. In addition to the general structural features of GCPII, we discuss how the detailed knowledge of protein-inhibitor/protein-substrate interactions contributes to the rational design of novel compounds, and, to some extent, helps to elucidate physiological functions of the enzyme.

2. HISTORY

The gene encoding human GCPII is located on chromosome 11 at the position 11p11.2 and includes 19 exons. The exon-intron structure of GCPII is associated with the emergence of several GCPII splice variants [13]. The full-length human GCPII, belonging to the class II transmembrane glycoproteins, comprises 750 amino acids and at the plasma membrane is present in the form of a homodimer.

Cloning of the GCPII gene from several species [14-18] allowed detailed analysis of the sequence and led to the assignment of GCPII to the MEROPS M28 peptidase family of co-catalytic metallopeptidases [19]. This rather diverse protein family includes among others aminopeptidases S (*Streptomyces gryseus*) and Ap1 (*Vibrio proteolytica*) as well as transferrin receptors. Based on sequence homology within the M28 family, Rawlings and Barret [20] set out to predict the domain structure of GCPII, to assign the active-site zinc ligands and to identify substrate-binding residues of GCPII. These predictions provided invaluable information for subsequent experimental studies of GCPII.

The assignment of GCPII into the M28 peptidase family encouraged work on 3D homology models of GCPII based on *Vibrio* aminopeptidase and transferrin receptor structures [21,22]. Although inspiring, these models have brought limited advancements to the field, mainly due to low sequence homology among the proteins as well as unforseen complexities in the architecture of the GCPII substrate-binding cavity. The real breakthrough in GCPII structural studies came only after the solution of experimental X-ray structures of the GCPII ectodomain by two independent groups in 2005 [23,24]. The experimental structures confirmed structural similarity to transferrin receptor, defined the nature of the dimerization interface, and revealed that the ectodomain of GCPII is composed of three intertwined domains. In addition, the series of higher resolution structures of GCPII complexes with several inhibitors reported by Mesters *et al.* [24] detailed the architecture of the GCPII specificity pocket including enzyme-substrate/inhibitor interactions and its induced-fit mechanism of substrate recognition. To date, 32 structures of GCPII complexes and 4 GCPIII complexes have been determined (Table **1** and Fig. **1**), with the highest resolution of 1.29 Å and 1.5 Å for GCPIII and GCPII, respectively. These structures, together with extensive site-directed mutagenesis and modeling studies enabled deeper understanding of the enzyme reaction mechanism and facilitated the rational design of novel inhibitors [7,25-28].

3. OVERALL FOLD, N-LINKED GLYCANS AND INORGANIC IONS

GCPII structural information, as detailed in the subsequent chapters, is available for the extracellular part of the protein (ectodomain; amino acids 44 – 750) only (Fig. **2**). While the N-terminal intracellular GCPII tail (amino acids 1 – 18) is unlikely to have any stable structural fold, the transmembrane part anchoring the protein to the plasma membrane (amino acids 19 – 43) almost certainly conforms to the α-helical topology typical for membrane-spanning protein segments [20]. However, there are no experimental data confirming these predictions.

The extracellular portion of GCPII comprises the protease-like domain (amino acids 57-116 and 352-590), the apical domain (amino acids 117-351), and the C-terminal domain (amino acids 591-750), and amino acid residues shaping the substrate binding cavity originate from all three domains [24]. The architecture of the protease-like domain featuring the seven-stranded mixed β-sheet,

*Address correspondence to this author at the Institute of Biotechnology AS CR, v.v.i., Laboratory of Structural Biology, Videnska 1083, 14200 Praha 4, Czech Republic; Tel: +420-296-443-615; Fax: +420-296-443-610; E-mail: cyril.barinka@img.cas.cz

0929-8673/12 $58.00+.00

Table 1. GCPII/GCPIII Structures Available at the RCSB

PDB code	Major Findings	Fig. caption	Resol.	Ref.
1Z8L	Overall GCPII fold; domain organization		3.50 Å	[23]
2C6P	As 1Z8L; definition of specificity pockets; importance of N-glycosylation for dimerization; induced-fit enzymatic mechanism; identification of Ca^{2+} and Cl^- ions in the structure; interactions with phospho(i)nate ZBGs	I1	2.39 Å	[24]
2C6G		I3	2.20 Å	
2C6C		I2	2.00 Å	
2OOT	Novel crystallization conditions; first "high-resolution" structure		1.64 Å	[51]
2PVW	Detailed architecture of the pharmacophore pocket; binding of glutamate(like) moieties; flexibility of Asn257	I6	1.71 Å	[61]
2PVV		I5	2.11 Å	
2OR4		I4	1.62 Å	
2JBK	Binding of glutamate(like) moieties in the pharmacophore pocket	I4	2.99 Å	[60]
2JBJ		I6	2.19 Å	
3BI0	Details of the S1 pocket and specificity for P1 acidic moieties; arginine patch flexibility; identification of the entrance lid	I7	1.67 Å	[31]
3BHX		I9	1.60 Å	
3BI1		I8	1.50 Å	
3D7H	GCPII interactions with urea-based inhibitors; identification of the S1 accessory hydrophobic pocket	I11	1.55 Å	[45]
3D7G		I12	1.75 Å	
3D7F		I13	1.54 Å	
3D7D		I10	1.69 Å	
3BXM	The first structure with the GCPII physiological substrate; detailed description of reaction mechanism	S1	1.71 Å	[25]
3IWW	Flexibility of the pharmacophore pocket at the Leu259-Asn262 segment	I11	2.3 Å	[54]
2XEJ	Identification of the arene-binding site	I19	1.78 Å	[41]
2XEI		I16	1.69 Å	
2XEG		I17	1.59 Å	
2XEF		I18	1.59 Å	
3SJX	GCPII complexes with an inhibitor and substrates with enhanced lipophilicity	S4	1.66 Å	[66]
3SJG		S2	1.65 Å	
3SJF		I14	1.65 Å	
3SJE		S3	1.70 Å	
3RBU	N-terminally Avi-tagged GCPII	I6	1.60 Å	[72]
3FEC	First structures of GCPIII		1.49 Å	[71]
3FED		I7	1.29 Å	
3FEE		I4	1.56 Å	
3FF3		I3	1.37 Å	

surrounded by 10 α-helices resembles most closely the fold of aminopeptidases from *Aeromonas proteolytica* [29] and *Streptomyces griseus* [30]. Within the relatively rigid scaffold of the protease-like domain a highly flexible segment of amino acids Trp541-Gly548 forms the so-called "entrance lid", which can control communication between the extracellular milieu and the interior (the substrate binding cavity) of the enzyme [31].

The apical domain is inserted between the first and the second β-sheet of the protease-like domain and consists of the central (3+4) stranded β-sandwich flanked by 4 α-helices. Following the β3 strand, of the polyproline type-2 helix made up of four consecutive proline residues (Pro146-Pro149) has been identified in the structure (Fig. **2A1**; [24]). This motif is generally involved in protein-protein interactions *via* its interaction with cognate SH3 (src-homology 3) modules [32]. Even though such interactions might be important for GCPII functioning as a receptor (ligands still not identified), it remains to be seen whether or not this motif really plays any physiological role.

The C-terminal domain (also called the helical domain) is formed by an Up-Down-Up-Down four helix bundle comprising helices α15, α17, α18-α19, α20, and a small helix α16 which is oriented perpendicularly to the previous ones. Two loops are inserted between helices α18 and α19: the first loop (amino acids Leu679-Val690) interacts with the protease-like domain, while the second, the β15/β16-hairpin loop ("glutarate sensor"; amino acids Tyr692-Ser704) reaches to the active site and engages a substrate/inhibitor molecule in the pharmacophore (S1') pocket. This sensor loop undergoes remarkable changes during the process of the substrate/inhibitor binding, and its movement is a prime example of the "induced fit" mechanism of substrate recognition [24]. (Fig. **3**)

The primary sequence of human GCPII harbors 10 potential N-glycosylation sites localized to Asn51, Asn76, Asn121, Asn140, Asn153, Asn195, Asn336, Asn459, Asn476, and Asn638, and carbohydrates can make up to 25% of the total molecular weight of the enzyme [33,34]. It has been shown that N-glycosylation has a profound effect on several biological/biophysical GCPII characteristics, including stability, proteolytic activity, apical sorting, association with lipid rafts, and proteolytic resistance [35-38]. As saccharide moieties are quite flexible, they are often not

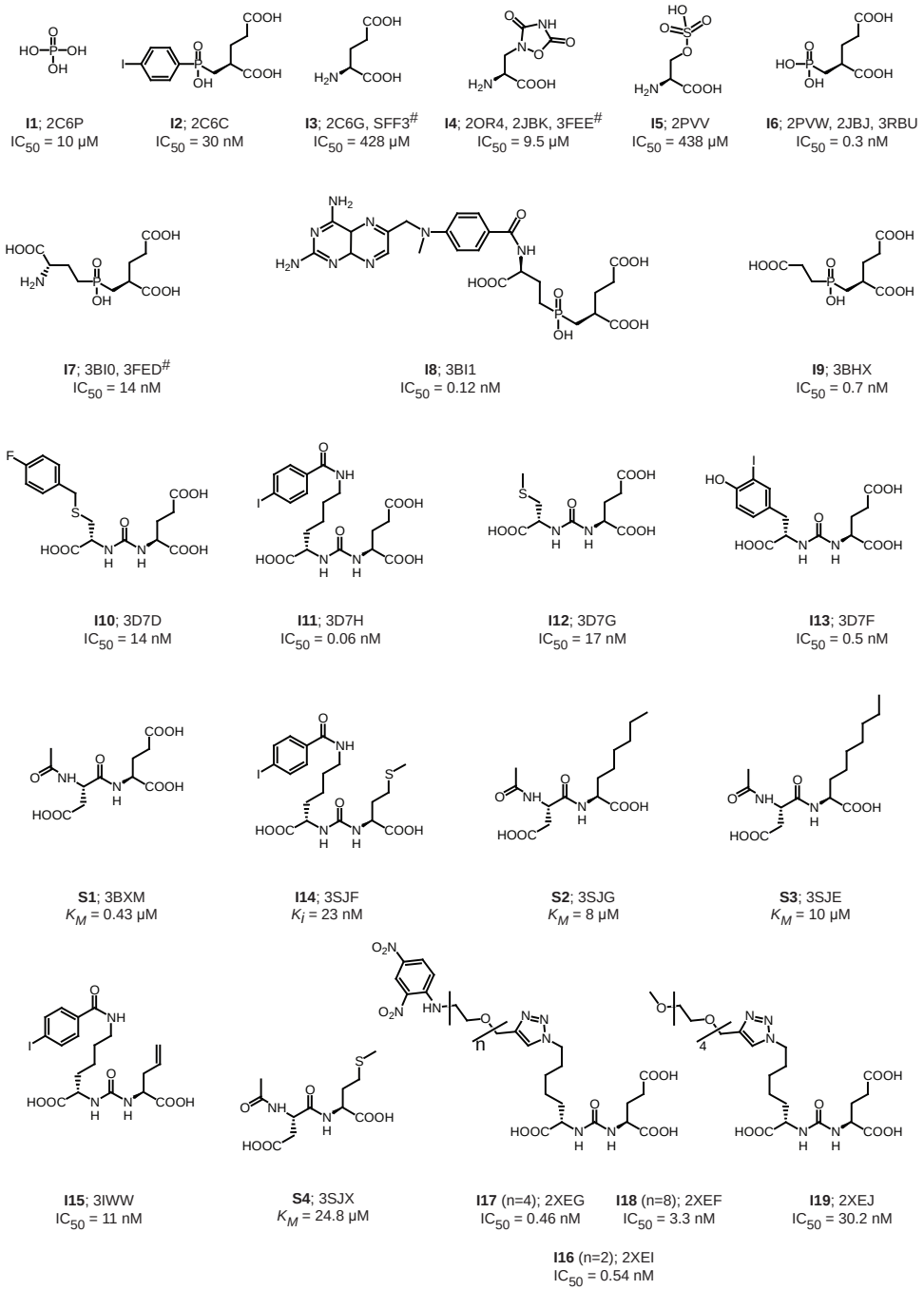

Fig. (1). Formulas of inhibitors and substrates in complexes with GCPII and GCPIII (GCPIII marked with #) as listed in Table 1.

Each compound is listed together with the corresponding PDB code(s) and the inhibition (IC_{50} or K_i) or Michaelis (K_M) constant for inhibitors and substrates, respectively. Data come from references [41,45,52,53,56,61,65].

seen in the electron density maps. In the case of GCPII, only one to two proximal saccharide units at each glycosylation site are typically visible in crystal structures, with the noticeable exception of the oligosaccharide chain attached to Asn638, where four saccharide units can be modeled in the electron density. Site-directed mutagenesis suggests that N-glycosylation at this position is indispensable for GCPII enzymatic activity [39] and structural data provides mechanistic explanation for this observation. The Asn638 oligosaccharide chain located at one monomer interacts with the side chains of Glu276 and Arg354 of the second GCPII monomer thus contributing to dimer formation (Fig. **2C1**). Since the dimerization is required for proteolytic activity, this rare, structurally well-defined example of protein-carbohydrate interaction can be viewed as a stabilization factor in GCPII dimerization with direct implications to the GCPII proteolytic activity.

There are four inorganic ions present in the GCPII structure – two active-site zincs, one chloride anion and one calcium cation [24]. The active site zincs play both a functional and a structural role and their importance will be detailed in the following sections. The calcium ion (at the distance of 20 Å from the active-site) is coordinated by amino acids Glu433, Glu436, Thr269, and Tyr272 at the interface of the protease-like and apical domains and its role

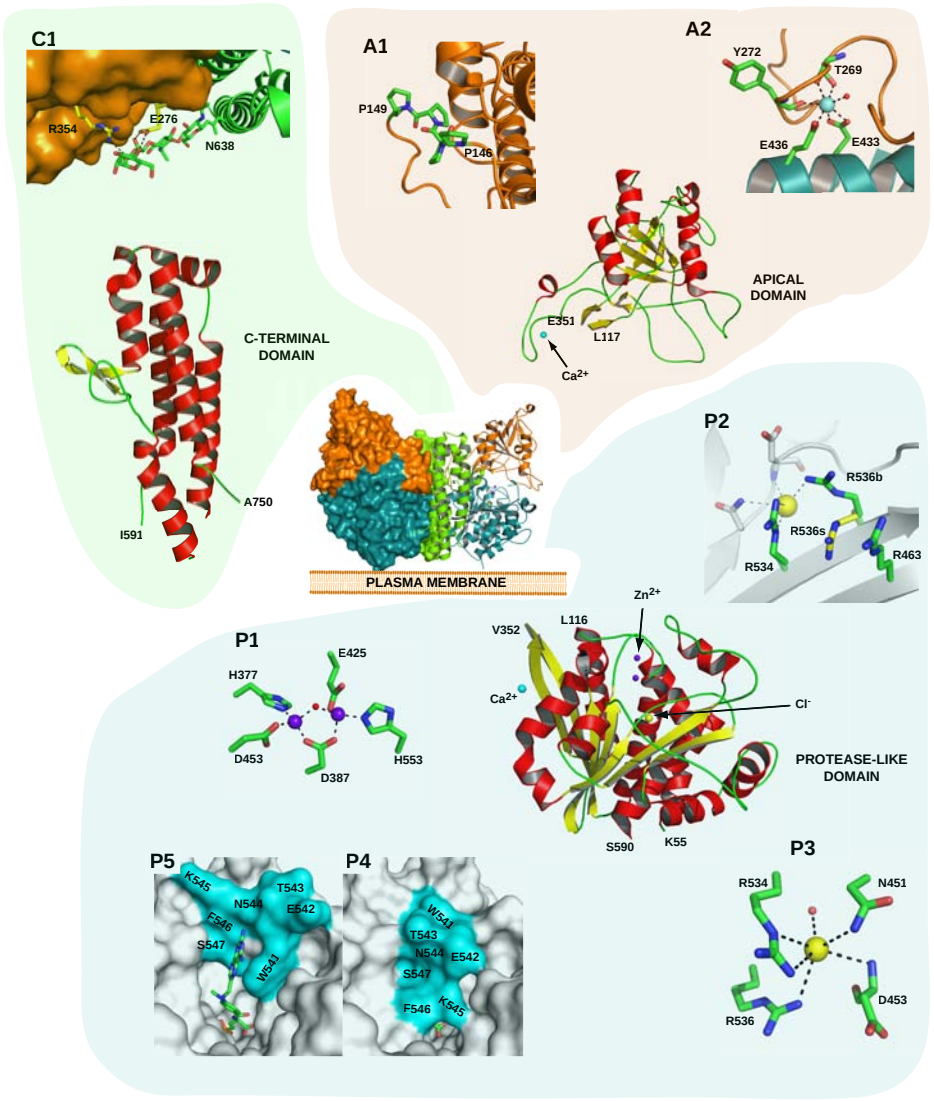

Fig. (2). Selected structural features of human GCPII.

GCPII homodimer in the center of the figure with one monomer shown in surface representation and the second as cartoon. Individual domains of the extracellular part colored cyan (protease-like domain; amino acids 57-116 and 352-590), orange (apical domain; amino acids 117-351), and green (C-terminal; amino acids 591-750). The cartoon representations of individual isolated domains are also shown within shaded areas with α-helices, β-strands, and loops colored red, yellow, and green, respectively. Details of important structural features for the individual domains: **C1**, the detailed view of protein-carbohydrate interactions in the GCPII structure. An oligosaccharide chain anchored at the Asn638 side chain (green sticks) of the first monomer (green cartoon) interacts with the side chains of Glu276 and Arg354 (yellow sticks) of the second GCPII monomer (orange surface) thus contributing to dimer formation. Hydrogen bonding interactions are shown as dashed lines. **A1**, the solvent exposed type-II polyproline helix (Pro146–Pro149); a signature motif that is typically implicated in the intermolecular contacts *via* its interaction with src-homology 3 modules. **A2**, the detailed architecture of the calcium-binding site. Residues from the apical (Tyr272 and Thr269) and the protease-like (Glu433 and Glu436) domains contribute to the Ca^{2+} (cyan sphere) coordination sphere. This motif is involved in GCPII dimerization by stabilizing the loop 272–279 at the dimerization interface. **P1**, the coordination sphere of active site zinc ions (purple spheres). **P2**, flexibility of the arginine patch residues. Side chains of the arginine patch (Arg534, Arg536, and Arg463) are shown in stick representation, the chloride ion as a yellow sphere. While the side chain of Arg534 is virtually immobile, the Arg536 side chain can adopt two conformations depending on the occupancy of the S1 site – the binding conformation (R536b, green) and stacking conformation (R536s, yellow) with the S1 site empty or occupied, respectively. **P3**, the coordination sphere of the chloride anion (yellow sphere). **P4, 5**, the entrance lid (Trp541-Gly548) in the closed (**P4**) and open (**P5**) conformation. GCPII is shown in surface representation with the entrance lid colored cyan.

seems to be the stabilization of the Tyr272-Tyr279 loop, which is involved in dimerization of the enzyme (Fig. **2A2**). The negatively charged chloride ion is located in the vicinity of the arginine patch and its coordination sphere includes Arg534, Arg536, Asn451, and Asp453. It is believed to be implicated in the positioning of positively charged residues, namely Arg534, that are intimately involved in substrate/inhibitor interactions and contribute to GCPII substrate specificity and/or inhibitor affinity (Fig. **2P3**).

4. SUBSTRATE BINDING CAVITY AND ADJACENT STRUCTURAL MOTIFS

The internal cavity (or substrate/inhibitor binding cavity) of GCPII resembles an irregularly shaped funnel terminated at the bottom by a bulging pharmacophore pocket (Fig. **3**). The funnel opening at the surface of the protein with an approximate diameter of 20 Å is shaped by residues stemming from all three extracellular domains, as is the wall of the 20 Å deep funnel that leads into the

active site marked by the presence of two zinc ions. The following paragraphs offer a more detailed picture of individual parts of the GCPII internal cavity together with their importance for GCPII functioning and inhibitor design.

4.1. Entrance Lid and Arene-Binding Site

The GCPII internal pocket can be shielded from the external space by the entrance lid – a flexible loop comprising amino acids Trp541-Gly548 (Fig. **2P4,5**). Crystallographic studies revealed two major conformations of the lid – open and closed – and the transition between the two is enabled by flipping of the peptide bond between Asn540 and Trp541 at one hinge and flexibility of Gly548 at the other [40]. In closed conformation the entrance lid forms a single turn α-helix precluding communication between the enzyme interior and the external space. On the other hand, the open conformation is observed in GCPII complexes with inhibitors featuring extended P1 moieties (e.g. a transition state analog of folyl-γ-glutamate, antibody recruiting molecules), where the closed conformation would be sterically prohibited due to the interference of bulky inhibitor moieties [40,41]. As GCPII is able to process "long" substrates, such as folyl-poly-γ- glutamates, [42,43] it can be

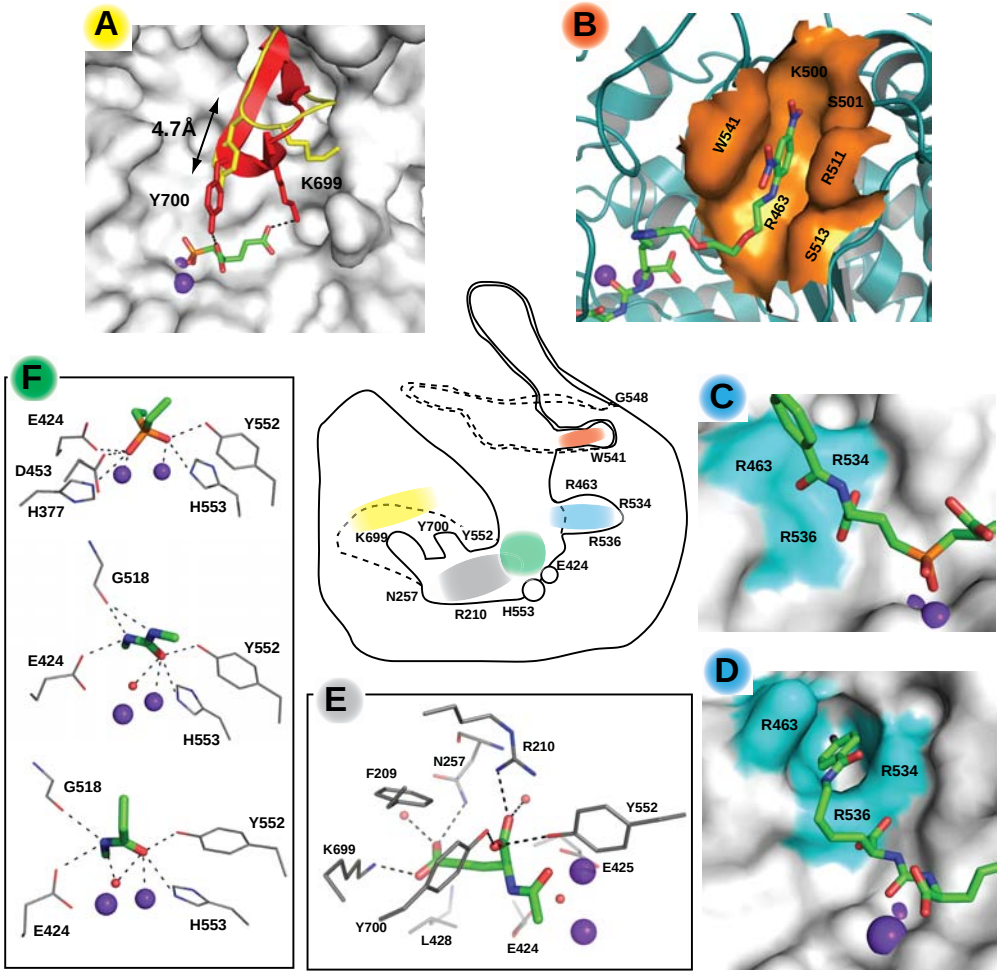

Fig. (3). The internal cavity of human GCPII.

The schematic representation of GCPII in the center of the figure. Flexible segments (the entrance lid, the arginine patch and the glutarate sensor) are depicted in two conformations by solid and dashed lines, respectively. Selected residues lining the internal cavity are shown in one-letter code and the approximate positions for associated representations of structural details (Panels **A** through **F**) are color-coded. Zinc atoms are depicted as circles. Clockwise: **A**; the position of the glutarate sensor, when the pharmacophore pocket is empty (yellow) or occupied by an inhibitor/substrate (red). Note the positional difference of 4.7 Å (for C-α atoms of Y700) between the two conformations of the glutarate sensor. The dissected internal GCPII cavity is shown in surface representation, S1'-bound inhibitor (2-PMPA) in sticks (PDB code 2PVW). **B**; the details of the arene-binding site occupied by the dinitrophenyl group of ARM-P2 (PDB code 2XEI). The arene-binding site is shown in surface representation and colored in orange. **C**; the surface representation of the arginine patch (cyan) in the "stacking conformation". The existence of the arginine patch is responsible for the enzyme preference for acidic groups at the P1 position of substrates/inhibitors (pdb code 3BI1). **D**; the S1 accessory hydrophobic pocket (approximate dimensions of 8.5 Å x 7 Å x 9 Å) is opened by simultaneous repositioning of the side chains of Arg463 and Arg536. The pocket can accommodate suitable distal parts of inhibitors contributing thus to the tighter inhibitor binding. GCPII shown in surface representation, the DCIBzL inhibitor as sticks (PDB code 3D7H). **E**; hydrogen-bonding interactions between the S1' (pharmacophore) pocket-bound substrate and interacting GCPII residues. The selectivity of GCPII towards glutamate and glutamate-like compounds is achieved *via* an intricate network of both polar and non-polar interactions. **F**; interactions in the vicinity of the active-site zinc ions. Phosphinate (top) and urea (middle) zinc-binding groups contribute markedly to the affinity of inhibitors towards GCPII. The peptide bond of NAAG (bottom) shown for comparison. Zinc ions and water molecules are shown as purple and red spheres, respectively. Inhibitors/substrates bound are in stick representation with carbon atoms colored green, while GCPII residues are shown as lines with carbon atoms colored gray (panels E and F). Remaining atoms are colored blue (nitrogen), red (oxygen), and orange (phosphorus). Hydrogen-bonding interactions are shown as dashed lines.

inferred that the ability of the enzyme to hydrolyze its substrate does not depend on the position of the entrance lid throughout the catalytic cycle.

In relation to the inhibitor design, it is interesting to note that in its open conformation the entrance lid can be exploited for the design of ultra-high affinity GCPII inhibitors [41]. While mapping interactions between GCPII and antibody-recruiting molecules targeting prostate cancer (ARM-Ps), we recently identified and characterized a simple structural motif termed the arene-binding site comprising amino acids Arg463, Arg511, and Trp541. ARM-Ps consist of a glutamate-urea docking module linked to a dinitrophenyl group (DNP) *via* an oxyethylene linker, and the presence of the DNP increases the total inhibitory potency of ARM-Ps up to 60-fold. An increase of inhibitor affinity for GCPII is due to avidity effect as the DNP engages residues forming the arene-binding site, with the most important being stacking interactions with the side chain of Trp541, a residue of the entrance lid [41] (Fig. **3B**).

4.2. Non-Pharmacophore Site and the Arginine Patch

The term "non-pharmacophore site" of GCPII as used herein is defined quite loosely and encompasses basically the whole funnel from its narrow (approximately 8 Å) base at the active-site zincs to the funnel rim or entrance lid residues in closed conformation. Given variable physicochemical characteristics of residues lining the non-pharmacophore site together with its sizeable dimensions it is not surprising that this part of the internal GCPII cavity is viewed as much less restrictive (compared to the pharmacophore pocket; see below) and more amenable to modifications of the distal functionalities (D-moieties) of GCPII-specific inhibitors [7,41,44-50].

The most conspicuous feature of the non-pharmacophore site is an extended, positively charged surface area termed the arginine patch that is defined by the apposition of guanidinium groups of Arg534, Arg536, and Arg463 (all located within antiparallel β-strands β13 and β14) [24,51] (Fig. **3C**). The existence of this patch provides a mechanistic explanation for the preference of GCPII for acidic residues at the P1 position of a substrate [52,53]. In addition, interactions between the patch of arginines and negatively charged functionalities of inhibitors contribute substantially to the inhibitor affinity towards GCPII. Not surprisingly, the majority of GCPII small-molecule ligands feature a negatively charged group at the P1 position to take the advantage of this fact.

The arginine patch architecture is supported by the presence of a chloride ion that stabilizes the side chain of Arg534 in an invariant (though energetically unfavorable) 'all-gauche' conformation. On the other hand, structural studies document positional variability of the two remaining arginine side chains (Arg536 and Arg463) and their importance for inhibitor design. In the ligand-free form of the enzyme, the three arginines are 'stacked' on top of each other [51], but the situation looks different when a ligand (inhibitor or substrate) is bound. Here, Arg536 typically adopts 'binding' conformation by repositioning its guanidinium group by 4.5 Å [31] (Fig. **2P2**). Together with the simultaneous relocation of the Arg463 side chain, a new (previously cryptic) hydrophobic pocket of dimensions 7 Å x 8.5 Å x 9 Å is formed (Fig. **3C,D**). The iodo-benzyl group of DCIBzL, a urea-based imaging compound, closely fits into the pocket, substantially decreasing the inhibition constant of DCIBzL for GCPII [45]. The "S1-accessory hydrophobic pocket" (together with the arene-binding site) is the prime example of GCPII structural plasticity. The existence and importance of similar "cryptic sites" should not be underestimated during the structure-activity relationship studies [45,54].

It is likely that given the substantial variability of D-moieties of GCPII-specific inhibitors, future studies are going to uncover the importance of the hitherto unnoticed structural features of the non-pharmacophore pocket that can be used for the design of novel GCPII inhibitors. Taking into account the size and variability, the non-pharmacophore pocket is therefore well suited for the development of future GCPII-specific ligands.

4.3. The Active Site, Enzymatic Mechanism and Zinc-Binding Groups

The active site of GCPII, which separates non-pharmacophore and pharmacophore pockets, is centered around two zinc ions: the catalytic Zn^{2+} is coordinated by His553 and Glu425, while the co-catalytic Zn^{2+} is engaged by the side chains His377 and Asp453 (the only zinc binding residue shared with the transferrin receptor). The Asp387 side chain bridges both zincs in a bidentate fashion (Fig. **2P1**). Crucial for the GCPII enzymatic properties is also the presence of the bridging hydroxide anion (at the distance of 1.79 Å and 2.26 Å from the co-catalytic and catalytic zinc, respectively) and the Glu424 proton shuttle [25].

Crystallographic studies provided snapshots (ligand-free structure, complexes with the intact substrate, the tetrahedral intermediate, and the reaction product) of the GCPII active-site (re)arrangement during the hydrolytic cycle of the enzyme, and these data, together with quantum mechanics/molecular mechanics calculations allowed us to reconstruct the catalytic mechanism of the enzyme [25]. In a simplified view, the carbonyl group of the scissile peptide bond of N-acetyl-L-aspartyl-L-glutamate (NAAG) is polarized *via* its interaction with the catalytic zinc and the carbonyl carbon atom attacked by the bridging hydroxide anion. The resulting tetrahedral intermediate is stabilized by interactions with both zinc ions (now 0.5 Å farther apart than in the ligand-free structure) as well as residues surrounding the active site. At the same time, the proton extracted from the bridging water molecule is shuttled through the Glu424 side chain to the amide nitrogen of the scissile peptide bond resulting in its breakdown and release of the reaction products. The reaction cycle is completed by the influx of a water molecule to the bridging position. The bridging water immediately loses one of its protons (to the Glu424 side chain) and the enzyme is prepared for the subsequent hydrolytic cycle (Fig. **4**).

The active-site zincs are not only crucial for the enzymatic properties of GCPII, but are also instrumental for the design of high-affinity GCPII inhibitors. In fact, every high-affinity GCPII inhibitor features a zinc-binding group (ZBG) in the structure and the attachment of a ZBG to a common structural motif (such as glutarate moiety) increases its affinity many folds. The prime examples can be 2-MPPA [2-(3-mercaptopropyl)pentanedioic acid] and 2-PMPA (2-phosphonomethylpentanedioic acid), thiol and phosphonate containing analogs of glutamate, with an increase in potency of approximately 10^4-fold and 10^6-fold, respectively [55,56]. In addition to thiols and phosphonates, several other ZBGs are employed in the inhibitor design, including hydroxamates, phosphinates, phosphoamidates, ureas, and sulfonamides [47,49,57-59]. At present, structural information is available only for three ZBGs and their interactions with GCPII – phosphonates, phosphinates, and ureas [24,40,41,45,60,61] (Fig. **3F**).

The binding mode at the GCPII active site is virtually identical for both phosphorus-containing groups. They mimic a tetrahedral reaction intermediate and structures of GCPII/phosphinate complexes were instrumental for the elucidation of the GCPII reaction mechanism. Two oxygen atoms of the phosphinate surrogate coordinate the active-site Zn^{2+} ions with the Zn…O distances of approximately 2.1 Å. One of the oxygens, replacing the bridging water molecule, further interacts with side chains of Glu424, Asp453, and His377, while the second is engaged by the side chains of Tyr552 and His553. The extensive network of GCPII/phospho(i)nate interactions contributes prominently to the high affinity of phosphorus-containing ligands for GCPII [61].

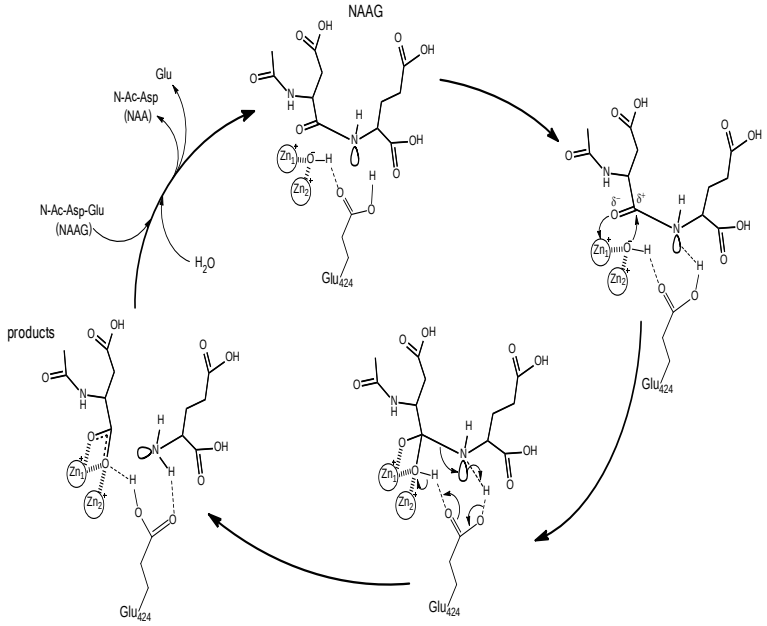

Fig. (4). Peptide bond hydrolysis catalyzed by GCPII.

The mechanism of peptide bond hydrolysis catalyzed by GCPII. Enzymatic hydrolysis of NAAG is schematically depicted in four basic steps. Substrate/products are shown in bold lines. Catalytic zinc ions are circled (Zn_1 is catalytic and Zn_2 cocatalytic) and electrons shifts are depicted by small arrows.

The urea-based inhibitors were introduced by Kozikowski group in 2004 [48] and the ureido group mimics a planar peptide bond of a GCPII substrate. The ureido carbonyl oxygen is engaged by the side chains of Tyr552 and His553 and further interacts with the bridging water molecule and the catalytic Zn^{2+}. One of the ureido nitrogens is H-bonded to Glu424, Gly518, and the bridging water molecule, while the second ureido nitrogen donates a hydrogen bond to the Gly518 main-chain carbonyl. Several urea-based inhibitors are being tested in clinical trials for prostate cancer imaging at present [62,63].

Although the ZBGs are known to be indispensable constituents of high-affinity GCPII inhibitors, their chemical diversity as well as the amount of structural information is surprisingly quite limited. In this respect, it might be advantageous to partly focus future studies on the identification and validation of alternative ZBGs with superior pharmacological properties.

4.4. The Pharmacophore (S1') Pocket

Concerning the development of GCPII-specific inhibitors, the pharmacophore (S1') pocket is undisputedly the most important portion of the GCPII internal cavity and as such it is reasonably well characterized by different experimental approaches including site-directed mutagenesis, X-ray crystallography, quantum mechanics/molecular mechanics calculations, and structure-activity relationship studies. The pocket of approximate dimensions 8 x 8 x 8 Å is located at the bottom of the internal GCPII cavity and is shaped by Phe209, Arg210, Asn257, Glu424, Glu425, Gly427, Leu428, Gly518, Lys699, and Tyr700. The plasticity of this pharmacophore pocket is somewhat limited, with the notable exception of the glutarate sensor (amino acids Tyr692-Ser704) which can withdraw from the S1' pocket by more than 4 Å, increasing its dimensions substantially [24,61].

The amphipathic pharmacophore pocket shows a strong preference for glutamate and glutamate-like moieties and to a large extent determines selectivity, specificity and affinity of GCPII towards small-molecule ligands/substrates. It is therefore not surprising that physiological GCPII substrates feature the glutamate moiety at the C-terminus and that the majority of GCPII-specific inhibitors are glutamate derivatives. Glutamate selectivity of the pharmacophore pocket is secured by an intricate network of polar (hydrogen bonding and ionic) interactions with the enzyme residues. The glutamate α-carboxylate group directly interacts with the guanidinium group of Arg210 and the hydroxyl groups of Tyr552 and Tyr700. Furthermore, it is engaged in water-mediated contacts with Asn257 and Arg210. The site-directed mutagenesis revealed a prominent role of Arg210 (and its interactions with α-carboxylate of a substrate/inhibitor) in substrate/inhibitor binding as mutations targeting this residue decreased GCPII affinity towards 2-PMPA by more than five orders of magnitude [26]. The γ-carboxylate group of S1'-bound glutamate accepts a hydrogen bond from the amide group of Asn257, forms salt bridge with the N^{ζ} group of Lys699, and also engages both these residues *via* a water molecule bridge [24,60,61] (Fig. **3E**).

Even though polar interactions between GCPII and pharmacophore pocket-bound ligands seem to be pivotal, non-polar (hydrophobic, van der Waals) interactions are an additional and a very important factor helping to accommodate and stabilize the P1' functionality of a substrate/inhibitor in the pharmacophore pocket. Here, side chains of Phe209 and Leu428 play the most prominent role with a lesser contribution by Lys699, Asn257, Gly427, and Gly518 [61]. The importance of non-polar interactions can be prominent in the cases in which the ultimate goal is to develop compounds that are able to penetrate into CNS/PNS compartments. Such inhibitors would be instrumental for the therapy of neurologic disorders. Several groups attempted to develop compounds with increased lipophilicity by substituting the S1'-targeted glutarate functionality with more hydrophobic moieties [28,65-66]. Despite partial successes, however, no GCPII-specific inhibitors with sufficient blood-brain barrier penetration have been reported so far.

The pharmacophore pocket is quite unyielding and does not readily accommodate substitutions for glutamate at the P1' functionalities of inhibitors, as typically placing a non-glutamate functionality at the P1' position of an inhibitor markedly decreases its potency (as compared to its glutamate-containing counterpart). At the same time, however, the observed positional flexibility of the

individual side chains shaping the pocket (Asn257, Lys699) as well as conformational changes of entire segments of the protein (the glutarate sensor; Leu259-Asn262) offer the enzyme "a breathing space" indispensable for accepting structurally diverse compounds. Consequently, the pharmacophore pocket of GCPII still has an untapped potential for future SAR studies.

5. GCPII POLYMORPHISM AND ORTHOLOGS

The best studied single nucleotide GCPII polymorphism is the 1561 C→T variant that corresponds to the His475Tyr mutation at the protein level. Lower folate and higher homocysteine levels were detected in plasma samples of subjects carrying this mutation, pointing towards the connection of this polymorphism with hyperhomocysteinemia [67]. These findings were, however, questioned by other studies using bigger population samples [68,69]. Interestingly, the H475Y mutation was reported to decrease folylpoly-γ-carboxypeptidase activity of GCPII by approximately 50% *in vitro* [67]. As His475 is located approximately 17 Å and 25 Å from the arginine patch and the active-site, respectively, its influence on GCPII enzymatic activity is not obvious. Additionally, our unpublished structure of the H475Y variant does not reveal any structural perturbations that could be implicated in folate hydrolysis by GCPII. Further studies are required to detail and clarify the influence of GCPII polymorphism on folate metabolism/processing.

GCPII belongs to the transferrin receptor/glutamate carboxypeptidase II (TfR/GCPII) family, which encompasses both receptors and proteases; besides transferrin receptors TfR1 and TfR2 and GCPII homologs, it includes several GCPII orthologs: NAALADase L, NAALADase L2, GCPIII and PSMAL [71]. All members of this group seem to be evolutionary products of several gene duplication events. NAALADase L and NAALADase L2 are the most distant GCPII orthologs with sequence identities of 35% and 25% at the amino acid level, respectively. Neither of these enzymes is able to hydrolyze NAAG, the natural GCPII substrate, and their physiological role(s) is not known at present [70]. No structural information is available for either of the two proteins, but at least NAALADase L2 is unlikely to have an enzymatic activity similar to GCPII, since it lacks amino acids corresponding to residues forming the active site of GCPII, including the crucial zinc-binding residues.

PSMAL expression has been reported in kidney and liver and it shares 97% sequence identity with GCPII at the amino acid level. PSMAL lacks the first 306 residues of the full-length GCPII that encompass both intracellular and transmembrane GCPII parts, together with substantial portions of the extracellular protease and apical domains. Consequently, despite the high level of sequence identity between the two proteins, PSMAL (clearly) lacks the substrate specificity of GCPII and likely hydrolytic activity altogether [70].

GCPIII (also known as NAALADase 2) is the second best studied member of this family with 67% sequence identity to GCPII at the amino acid level. Both enzymes have similar substrate specificities as well as virtually identical pharmacologic profiles [53]. Crystal structures of several GCPIII complexes were reported by Hlouchova *et al.* in 2009 [71]. Given the high sequence similarity between human GCPII and GCPIII it is not surprising that the overall structure of both enzymes is nearly identical with root mean square deviation < 1 Å for equivalent C-α atoms. Likewise, the architecture of non-pharmacophore and pharmacophore pockets as well as identities of the surrounding amino acids (with the exception of Ser509 that is equivalent to Asn519 in human GCPII) are very similar, making a structurally-aided design of isoform specific inhibitors extremely challenging. One of the potential avenues to explore for the design of isoform specific compounds can be engaging the remote-binding sites in GCPII, such as the arene-binding pocket that is absent from the GCPIII structure. We believe, however, that pursuing isoform specific inhibitors warrants further studies, as such compounds would be instrumental in dissecting the physiological roles of the two isoforms.

6. PERSPECTIVES AND CONCLUDING REMARKS

Our understanding of GCPII structure-function relationship increased considerably during recent years, but many outstanding issues remain to be resolved. These include physiological aspects of GCPII (non-enzymatic role in healthy tissues and receptor-like properties, the existence of additional physiological ligands/substrates, signaling pathways, distinct role(s) of splice variants) as well as more basic structure-function questions (the exact role of dimerization and carbohydrates on enzymatic activity, effects of GCPII natural polymorphism, the plasticity of (non)-pharmacophore pockets of the enzyme in inhibitor design). Structural/modeling studies are an important part of such undertakings and can help in finding answers for both basic research-oriented problems as well as in rationalizing the development of drugs for clinical applications. The major challenges lay probably in the development of GCPII-specific blood-brain barrier permeable compounds that could be used for the treatment of neurological disorders associated with acute or chronic glutamate excitotoxicity. Hopefully, probing the enzyme with more diverse compounds will lead to the identification of novel structural features and therefore contribute to the rational design of drugs targeting GCPII.

ACKNOWLEDGEMENT

The financial support from EMBO (Installation grant #1978), Ministry of Education, Youth and Sports of the Czech Republic (ME10031), and the IBT (AV0Z50520701) institutional support are gratefully acknowledged. Jakub Ptacek is in part supported by the PhD fellowship from The Faculty of Natural Science, Charles University in Prague.

ABBREVIATIONS

ARM-Ps	=	antibody-recruiting molecules targeting prostate cancer
CNS	=	central nervous system
DNP	=	dinitrophenyl group
GCPII	=	glutamate carboxypeptidase II
NAAG	=	N-acetyl-L-aspartyl-L-glutamate
NAALADAse	=	N-acetylated-α-linked acidic dipeptidase
PNS	=	peripheral nervous system
PSMA	=	prostate-specific membrane antigen
ZBG	=	zinc-binding group

REFERENCES

[1] Zhou, J.; Neale, J.H.; Pomper M.G.; Kozikowski A.P. NAAG peptidase inhibitors and their potential for diagnosis and therapy. *Nat. Rev. Drug Discov.*, **2005**, *4*, 1015-1026.

[2] Bostwick, D.G.; Pacelli, A.; Blute, M.; Roche, P.; Murphy, G.P. Prostate specific membrane antigen expression in prostatic intraepithelial neoplasia and adenocarcinoma: a study of 184 cases. *Cancer*, **1998**, *82*, 2256-2261.

[3] Berger, U.V.; Carter, R.E.; McKee, M.; Coyle, J.T. N-acetylated alpha-linked acidic dipeptidase is expressed by non-myelinating Schwann cells in the peripheral nervous system. *J. Neurocytol.*, **1995**, *24*, 99-109.

[4] Sacha, P.; Zamecnik, J.; Barinka, C.; Hlouchova, K.; Vicha, A.; Mlcochova, P.; Hilgert, I.; Eckschlager, T.; Konvalinka, J. Expression of glutamate carboxypeptidase II in human brain. *Neuroscience*, **2007**, *144*, 1361-1372.

[5] Silver, D.A.; Pellicer, I.; Fair, W.R.; Heston, W.D.; Cordon-Cardo, C. Prostate-specific membrane antigen expression in normal and malignant human tissues. *Clin. Cancer Res.*, **1997**, *3*, 81-85.

[6] Slusher, B.S.; Vornov, J.J.; Thomas, A.G.; Hurn, P.D.; Harukuni, I.; Bhardwaj, A.; Traystman, R.J.; Robinson, M.B.; Britton, P.; Lu, X.C.; Tortella, F.C.; Wozniak, K.M.; Yudkoff, M.; Potter, B.M.; Jackson, P.F. Selective inhibition of NAALADase, which converts NAAG to glutamate, reduces ischemic brain injury. *Nat. Med.*, **1999**, *5*, 1396-1402.

[7] Tsukamoto, T.; Wozniak, K.M.; Slusher, B.S. Progress in the discovery and development of glutamate carboxypeptidase II inhibitors. *Drug Discov. Today*, **2007**, *12*, 767-776.

[8] Bander, N.H.; Nanus, D.M.; Milowsky, M.I.; Kostakoglu, L.; Vallabahajosula, S.; Goldsmith, S.J. Targeted systemic therapy of prostate cancer with a monoclonal antibody to prostate-specific membrane antigen. *Semin. Oncol.*, **2003**, *30*, 667-676.

[9] Bander, N.H. Technology insight: monoclonal antibody imaging of prostate cancer. *Nat. Clin. Pract. Urol.*, **2006**, *3*, 216-225.

[10] Chang, S.S.; Reuter, V.E.; Heston, W.D.; Bander, N.H.; Grauer, L.S.; Gaudin, P.B. Five different anti-prostate-specific membrane antigen (PSMA) antibodies confirm PSMA expression in tumor-associated neovasculature. *Cancer Res.*, **1999**, *59*, 3192-3198.

[11] Chang, S.S.; O'Keefe, D.S.; Bacich, D.J.; Reuter, V.E.; Heston, W.D.; Gaudin, P.B. Prostate-specific membrane antigen is produced in tumor-associated neovasculature. *Clin. Cancer Res.*, **1999**, *5*, 2674-2681.

[12] Milowsky, M.I.; Nanus, D.M.; Kostakoglu, L.; Sheehan, C.E.; Vallabhajosula, S.; Goldsmith, S.J.; Ross, J.S.; Bander, N.H. Vascular targeted therapy with anti-prostate-specific membrane antigen monoclonal antibody J591 in advanced solid tumors. *J. Clin. Oncol.*, **2007**, *25*, 540-547.

[13] O'Keefe, D.S.; Su, S.L.; Bacich, D.J.; Horiguchi, Y.; Luo, Y.; Powell, C.T.; Zandvliet, D.; Russell, P.J.; Molloy, P.L.; Nowak, N.J.; Shows, T.B.; Mullins, C.; Vonder Haar, R.A.; Fair, W.R.; Heston, W.D.W. Mapping, genomic organization and promoter analysis of the human prostate-specific membrane antigen gene. *Biochim. Biophys. Acta*, **1998**, *1443*, 113-127.

[14] Israeli, R.S.; Powell, C.T.; Fair, W.R.; Heston, W.D.W. Molecular-Cloning of A Complementary-Dna Encoding A Prostate-Specific Membrane Antigen. *Cancer Res.*, **1993**, *53*, 227-230.

[15] Carter, R.E.; Feldman, A.R.; Coyle, J.T. Prostate-specific membrane antigen is a hydrolase with substrate and pharmacologic characteristics of a neuropeptidase. *Proc. Natl. Acad. Sci. USA*, **1996**, *93*, 749-753.

[16] Bzdega, T.; Turi, T.; Wroblewska, B.; She, D.; Chung, H.S.; Kim, H.; Neale, J.H. Molecular cloning of a peptidase against N-acetylaspartylglutamate from a rat hippocampal cDNA library. *J. Neurochem.*, **1997**, *69*, 2270-2277.

[17] Halsted, C.H.; Ling, E.H.; Luthi-Carter, R.; Villanueva, J.A.; Gardner, J.M.; Coyle, J.T. Folylpoly-gamma-glutamate carboxypeptidase from pig jejunum. Molecular characterization and relation to glutamate carboxypeptidase II. *J. Biol. Chem.*, **1998**, *273*, 20417-20424.

[18] Luthi-Carter, R.; Barczak, A.K.; Speno, H.; Coyle, J.T. Molecular characterization of human brain N-acetylated alpha-linked acidic dipeptidase (NAALADase). *J. Pharmacol. Exp. Ther.*, **1998**, *286*, 1020-1025.

[19] Rawlings, N.D.; Tolle, D.P.; Barrett, A.J. MEROPS: the peptidase database. *Nucleic Acids Res.*, **2004**, *32*, D160-D164.

[20] Rawlings, N.D.; Barrett, A.J. Structure of membrane glutamate carboxypeptidase. *Biochim. Biophys. Acta*, **1997**, *1339*, 247-252.

[21] Rong, S.B.; Zhang, J.; Neale, J.H.; Wroblewski, J.T.; Wang, S.; Kozikowski, A.P. Molecular modeling of the interactions of glutamate carboxypeptidase II with its potent NAAG-based inhibitors. *J. Med. Chem.*, **2002**, *45*, 4140-4152.

[22] Mahadevan, D.; Saldanha, J.W. The extracellular regions of PSMA and the transferrin receptor contain an aminopeptidase domain: implications for drug design. *Protein Sci.*, **1999**, *8*, 2546-2549.

[23] Davis, M.I.; Bennett, M.J.; Thomas, L.M.; Bjorkman, P.J. Crystal structure of prostate-specific membrane antigen, a tumor marker and peptidase. *Proc. Natl. Acad. Sci. USA*, **2005**, *102*, 5981-5986.

[24] Mesters, J.R.; Barinka, C.; Li, W.X.; Tsukamoto, T.; Majer, P.; Slusher, B.S.; Konvalinka, J.; Hilgenfeld, R. Structure of glutamate carboxypeptidase II, a drug target in neuronal damage and prostate cancer. *EMBO J.*, **2006**, *25*, 1375-1384.

[25] Klusak, V.; Barinka, C.; Plechanovova, A.; Mlcochova, P.; Konvalinka, J.; Rulisek, L.; Lubkowski, J. Reaction Mechanism of Glutamate Carboxypeptidase II Revealed by Mutagenesis, X-ray Crystallography, and Computational Methods. *Biochemistry*, *48*, **2009**, 4126-4138.

[26] Mlcochova, P.; Plechanovova, A.; Barinka, C.; Mahadevan, D.; Saldanha, J.W.; Rulisek, L.; Konvalinka, J. Mapping of the active site of glutamate carboxypeptidase II by site-directed mutagenesis. *FEBS J.*, **2007**, *274*, 4731-4741.

[27] Grella, B.; Adams, J.; Berry, J.F.; Delahanty, G.; Ferraris, D.V.; Majer, P.; Ni, C.Y.; Shukla, K.; Shuler, S.A.; Slusher, B.S.; Stathis, M.; Tsukamoto, T. The discovery and structure-activity relationships of indole-based inhibitors of glutamate carboxypeptidase II. *Bioorg. Med. Chem. Lett.*, **2010**, *20*, 7222-7225.

[28] Wang, H.; Byun, Y.; Barinka, C.; Pullambhatla, M.; Bhang, H.E.; Fox, J.J.; Lubkowski, J.; Mease, R.C.; Pomper, M.G. Bioisosterism of urea-based GCPII inhibitors: Synthesis and structure-activity relationship studies. *Bioorg. Med. Chem. Lett.*, **2010**, *20*, 392-397.

[29] Chevrier, B.; Schalk, C.; Dorchymont, H.; Rondeau. J.M.; Tarnus, C.; Moras, D. Crystal-Structure of Aeromonas-Proteolytica Aminopeptidase - A Prototypical Member of the Co-Catalytic Zinc Enzyme Family. *Structure*, **1994**, *2*, 283-291.

[30] Greenblatt, H.M.; Almog, O.; Maras, B.; Spungin-Bialik, A.; Barra, D.; Blumberg, S.; Shoham, G. Streptomyces griseus aminopeptidase: X-ray crystallographic structure at 1.75 angstrom resolution. *J. Mol. Biol.*, **1997**, *265*, 620-636.

[31] Barinka, C.; Hlouchova, K.; Rovenska, M.; Majer, P.; Dauter, M.; Hin, N.; Ko, Y.S.; Tsukamoto, T.; Slusher, B.S.; Konvalinka, J.; Lubkowski, J. Structural basis of interactions between human glutamate carboxypeptidase II and its substrate analogs. *J. Mol. Biol.*, **2008**, *376*, 1438-1450.

[32] Kaneko, T.; Li, L.; Li, S.S. The SH3 domain--a family of versatile peptide- and protein-recognition module. *Front Biosci.*, **2008**, *13*, 4938-4952.

[33] Holmes, E.H.; Greene, T.G.; Tino, W.T.; Boynton, A.L.; Aldape, H.C.; Misrock, S.L.; Murphy, G.P. Analysis of glycosylation of prostate-specific membrane antigen derived from LNCaP cells, prostatic carcinoma tumors, and serum from prostate cancer patients. *Prostate*, **1996**, *7*, 25-29.

[34] Tiffany, C.W.; Lapidus, R.G.; Merion, A.; Calvin, D.C.; Slusher, B.S. Characterization of the enzymatic activity of PSM: Comparison with brain NAALADase. *Prostate*, **1999**, *39*, 28-35.

[35] Ghosh, A.; Heston, W.D.W. Effect of carbohydrate moieties on the folate hydrolysis activity of the prostate specific membrane antigen. *Prostate*, **2003**, *57*, 140-151.

[36] Barinka, C.; Sacha, P.; Sklenar, J.; Man, P.; Bezouska, K.; Slusher, B.S.; Konvalinka, J. Identification of the N-glycosylation sites on glutamate carboxypeptidase II necessary for proteolytic activity. *Protein Sci.*, **2004**, *13*, 1627-1635.

[37] Christiansen, J.J.; Rajasekaran, S.A.; Inge, L.; Cheng, L.; Anilkumar, G.; Bander, N.H.; Rajasekaran, A.K. N-glycosylation and microtubule integrity are involved in apical targeting of prostate-specific membrane antigen: implications for immunotherapy. *Mol. Cancer Ther.*, *4*, **2005**, 704-714.

[38] Castelletti, D.; Alfalah, M.; Heine, M.; Hein, Z.; Schmitte, R.; Fracasso, G.; Colombatti, M.; Naim, H.Y. Different glycoforms of prostate-specific membrane antigen are intracellularly transported through their association with distinct detergent-resistant membranes. *Biochem. J.*, **2008**, *409*, 149-157.

[39] Barinka, C.; Sacha, P.; Sklenar, J.; Man, P.; Bezouska, K.; Slusher, B.S.; Konvalinka, J. Identification of the N-glycosylation sites on glutamate carboxypeptidase II necessary for proteolytic activity. *Protein Sci.*, **2004**, *13*, 1627-1635.

[40] Barinka, C.; Hlouchova, K.; Rovenska, M.; Majer, P.; Dauter, M.; Hin, N.; Ko, Y.S.; Tsukamoto, T.; Slusher, B.S.; Konvalinka, J.; Lubkowski, J. Structural basis of interactions between human glutamate carboxypeptidase II and its substrate analogs. *J. Mol. Biol.*, **2008**, *376*, 1438-1450.

[41] Zhang, A.X.; Murelli, R.P.; Barinka, C.; Michel, J.; Cocleaza, A.; Jorgensen, W.L.; Lubkowski, J.; Spiegel, D.A. A Remote Arene-Binding Site on Prostate Specific Membrane Antigen Revealed by Antibody-Recruiting Small Molecules. *J. Am. Chem. Soc.*, **2010**, *132*, 12711-12716.

[42] Pinto, J.T.; Suffoletto, B.P.; Berzin, T.M.; Qiao, C.H.; Lin, S.; Tong, W.P.; May, F.; Mukherjee, B.; Heston, W.D. Prostate-specific membrane antigen: a novel folate hydrolase in human prostatic carcinoma cells. *Clin. Cancer Res.*, **1996**, *2*, 1445-1451.

[43] Luthi-Carter, R.; Barczak, A.K.; Speno, H.; Coyle, J.T. Hydrolysis of the neuropeptide N-acetylaspartylglutamate (NAAG) by cloned human glutamate carboxypeptidase II. *Brain Res.*, **1998**, *795*, 341-348.

[44] Banerjee, S.R.; Foss, C.A.; Castanares, M.; Mease, R.C.; Byun, Y.; Fox, J.J.; Hilton, J.; Lupold, S.E.; Kozikowski, A.P.; Pomper, M.G. Synthesis and evaluation of technetium-99m- and rhenium-labeled inhibitors of the prostate-specific membrane antigen (PSMA). *J. Med. Chem.*, **2008**, *51*, 4504-4517.

[45] Barinka, C.; Byun, Y.; Dusich, C.L.; Banerjee, S.R.; Chen, Y.; Castanares, M.; Kozikowski, A.P.; Mease, R.C.; Pomper, M.G.; Lubkowski, J. Interactions between Human Glutamate Carboxypeptidase II and Urea-Based Inhibitors: Structural Characterization. *J. Med. Chem.*, **2008**, *51*, 7737-7743.

[46] Foss, C.A.; Mease, R.C.; Fan, H.; Wang, Y.; Ravert, H.T.; Dannals, R.F.; Olszewski, R.T.; Heston, W.D.; Kozikowski, A.P.; Pomper, M.G. Radiolabeled small-molecule ligands for prostate-specific membrane antigen: *in vivo* imaging in experimental models of prostate cancer. *Clin Cancer Res*, **2005**, *11*, 4022-4028.

[47] Jackson, P.F.; Tays, K.L.; Maclin, K.M.; Ko, Y.S.; Li, W.; Vitharana, D.; Tsukamoto, T.; Stoermer, D.; Lu, X.C.; Wozniak, K.; Slusher, B.S. Design and pharmacological activity of phosphinic acid based NAALADase inhibitors. *J. Med. Chem.*, **2001**, *44*, 4170-4175.

[48] Kozikowski, A.P.; Zhang,J.; Nan, F.J.; Petukhov, P.A.; Grajkowska, E.; Wroblewski, J.T.; Yamamoto, T.; Bzdega, T.; Wroblewska, B.; Neale, J.H. Synthesis of urea-based inhibitors as active site probes of glutamate carboxypeptidase II: Efficacy as analgesic agents. *J. Med. Chem.*, **2004**, *47*, 1729-1738.

[49] Liu, T.; Toriyabe, Y.; Kazak, M.; Berkman, C.E. Pseudoirreversible inhibition of prostate-specific membrane antigen by phosphoramidate peptidomimetics. *Biochemistry*, **2008**, *47*, 12658-12660.

[50] Liu, T.; Wu, L.Y.; Choi, J.K.; Berkman, C.E. *In vitro* targeted photodynamic therapy with a pyropheophorbide--a conjugated inhibitor of prostate-specific membrane antigen. *Prostate*, **2009**, *69*, 585-594.

[51] Barinka, C.; Starkova, J.; Konvalinka, J.; Lubkowski, J. A high-resolution structure of ligand-free human glutamate carboxypeptidase II. *Acta Crystallogr. Sect. F Struct. Biol. Cryst. Commun.*, **2007**, *63*, 150-153.

[52] Barinka, C.; Rinnova, M.; Sacha, P.; Rojas, C.; Majer, P.; Slusher, B.S.; Konvalinka, J. Substrate specificity, inhibition and enzymological analysis of recombinant human glutamate carboxypeptidase II. *J. Neurochem.*, **2002**, *80*, 477-487.

[53] Hlouchova, K.; Barinka, C.; Klusak, V.; Sacha, P.; Mlcochova, P.; Majer, P.; Rulisek, L.; Konvalinka, J. Biochemical characterization of human glutamate carboxypeptidase III. *J. Neurochem.*, **2007**, 101, 682-696.

[54] Wang, H.; Byun, Y.; Barinka, C.; Pullambhatla, M.; Bhang, H.E.; Fox, J.J.; Lubkowski, J.; Mease, R.C.; Pomper, M.G. Bioisosterism of urea-based GCPII inhibitors: Synthesis and structure-activity relationship studies. *Bioorg. Med. Chem. Lett.*, **2010**, *20*, 392-397.

[55] Majer, P.; Jackson, P.F.; Delahanty, G.; Grella, B.S.; Ko, Y.S.; Li, W.; Liu, Q.; Maclin, K.M.; Polakova, J.; Shaffer, K.A.; Stoermer, D.; Vitharana, D.; Wang, E.Y.; Zakrzewski, A.; Rojas, C.; Slusher, B.S.; Wozniak, K.M.; Burak, E.; Limsakun, T.; Tsukamoto, T. Synthesis and biological evaluation of thiol-based inhibitors of glutamate carboxypeptidase II: discovery of an orally active GCP II inhibitor. *J. Med. Chem.*, **2003**, *46*, 1989-1996.

[56] Jackson, P.F.; Cole, D.C.; Slusher, B.S.; Stetz, S.L.; Ross, L.E.; Donzanti, B.A.; Trainor, D.A. Design, synthesis, and biological activity of a potent inhibitor of the neuropeptidase N-acetylated alpha-linked acidic dipeptidase. *J. Med. Chem.*, **1996**, *39*, 619-622.

[57] Blank, B.R.; Alayoglu, P.; Engen, W.; Choi, J.K.; Berkman, C.E.; Anderson, M.O. N-substituted glutamyl sulfonamides as inhibitors of glutamate carboxypeptidase II (GCP2). *Chem. Biol. Drug Des.*, **2011**, *77*, 241-247.

[58] Kozikowski, A.P.; Nan, F.; Conti, P.; Zhang, J.; Ramadan, E.; Bzdega, T.; Wroblewska, B.; Neale, J.H.; Pshenichkin, S.; Wroblewski, J.T. Design of remarkably simple, yet potent urea-based inhibitors of glutamate carboxypeptidase II (NAALADase). *J. Med. Chem.*, **2001**, *44*, 298-301.

[59] Stoermer, D.; Liu, Q.; Hall, M.R.; Flanary, J.M.; Thomas, A.G.; Rojas, C.; Slusher, B.S.; Tsukamoto, T. Synthesis and biological evaluation of hydroxamate-based inhibitors of glutamate carboxypeptidase II. *Bioorg. Med. Chem. Lett.*, *13*, **2003**, 2097-2100.

[60] Mesters, J.R.; Henning, K.; Hilgenfeld, R. Human glutamate carboxypeptidase II inhibition: structures of GCPII in complex with two potent inhibitors, quisqualate and 2-PMPA. *Acta Crystallogr. D. Biol. Crystallogr.*, **2007**, *63*, 508-513.

[61] Barinka, C.; Rovenska, M.; Mlcochova, P.; Hlouchova, K.; Plechanovova, A.; Majer, P.; Tsukamoto, T.; Slusher, B.S.; Konvalinka, J.; Lubkowski, J. Structural insight into the pharmacophore pocket of human glutamate carboxypeptidase II. *J. Med. Chem.*, **2007**, *50*, 3267-3273.

[62] Hillier, S.M.; Maresca, K.P.; Femia, F.J.; Marquis, J.C.; Foss, C.A.; Nguyen, N.; Zimmerman, C.N.; Barrett, J.A.; Eckelman, W.C.; Pomper, M.G.; Joyal, J.L.; Babich, J.W. Preclinical evaluation of novel glutamate-urea-lysine analogues that target prostate-specific membrane antigen as molecular imaging pharmaceuticals for prostate cancer. *Cancer Res.*, **2009**, *69*, 6932-6940.

[63] Mease, R.C.; Dusich, C.L.; Foss, C.A.; Ravert, H.T.; Dannals, R.F.; Seidel, J.; Prideaux, A.; Fox, J.J.; Sgouros, G.; Kozikowski, A.P.; Pomper, M.G. N-[N-[(S)-1,3-Dicarboxypropyl]carbamoyl]-4-[18F]fluorobenzyl-L-cysteine, [18F]DCFBC: a new imaging probe for prostate cancer. *Clin. Cancer Res.*, **2008**, *14*, 3036-3043.

[64] Majer, P.; Hin, B.; Stoermer, D.; Adams, J.; Xu, W.; Duvall, B.R.; Delahanty, G.; Liu, Q.; Stathis, M.J.; Wozniak, K.M.; Slusher, B.S.; Tsukamoto, T. Structural optimization of thiol-based inhibitors of glutamate carboxypeptidase II by modification of the P1' side chain. *J. Med. Chem.*, **2006**, *49*, 2876-2885.

[65] Kozikowski, A.P.; Zhang, J.; Nan, F.; Petukhov, P.A.; Grajkowska, E.; Wroblewski, J.T.; Yamamoto, T.; Bzdega, T.; Wroblewska, B.; Neale, J.H. Synthesis of urea-based inhibitors as active site probes of glutamate carboxypeptidase II: efficacy as analgesic agents. *J. Med. Chem.*, **2004**, *47*, 1729-1738.

[66] Plechanovova, A.; Byun, Y.; Alquicer, G.; Skultetyova, L.; Mlcochova, P.; Nemcova, A.; Kim, H.J.; Navratil, M.; Mease, R.C.; Lubkowski, J.; Pomper, M.G.; Konvalinka, J.; Rulisek, L.; Barinka, C. Novel substrate-based inhibitors of human glutamate carboxypeptidase II with enhanced lipophilicity. *J. Med. Chem.*, **2011**, *54*, 7535-7546.

[67] Devlin, A.M.; Ling, E.H.; Peerson, J.M.; Fernando, S.; Clarke, R.; Smith, A.D.; Halsted, C.H. Glutamate carboxypeptidase II: a polymorphism associated with lower levels of serum folate and hyperhomocysteinemia. *Hum. Mol. Genet.*, **2000**, 9, 2837-2844.

[68] Lievers, K.J.A.; Kluijtmans, L.A.J.; Boers, G.H.J.; Verhoef, P.; den Heijer, M.; Trijbels, F.J.M.; Blom, H.J. Influence of a glutamate carboxypeptidase II (GCPII) polymorphism (1561C -> T) on plasma homocysteine, folate and vitamin B-12 levels and its relationship to cardiovascular disease risk. *Atherosclerosis*, **2002**, *164*, 269-273.

[69] Afman, L.A.; Trijbels, F.J.M.; Blom, H.J. The H475Y polymorphism in the glutamate carboxypeptidase II gene increases plasma folate without affecting the risk for neural tube defects in humans. *J. Nutr.*, **2003**, *133*, 75-77.

[70] Lambert, L.A.; Mitchell, S.L. Molecular evolution of the transferrin receptor/glutamate carboxypeptidase II family. *J. Mol. Evol.*, **2007**, *64*, 113-128.

[71] Hlouchova, K.; Barinka, C.; Konvalinka, J.; Lubkowski, J. Structural insight into the evolutionary and pharmacologic homology of glutamate carboxypeptidases II and III. *FEBS J.*, **2009**, *276*, 4448-4462.

[72] Tykvart, J.; Sacha, P.; Barinka, C.; Knedlik, T.; Starkova, J.; Lubkowski, J.; Konvalinka, J. Efficient and versatile one-step affinity purification of in vivo biotinylated proteins: Expression, characterization and structure analysis of recombinant human glutamate carboxypeptidase II. *Protein Expres. Purif.*, **2012**, *82*, 106-115.

Received: August 03, 2011 Revised: November 05, 2011 Accepted: November 07, 2011